PULSE-STREAM MODELS IN ARRAY IMAGING

Adrien Besson⋆, Dimitris Perdios⋆, Marcel Arditi⋆, Yves Wiaux∗, Jean-Philippe Thiran⋆,†

⋆Signal Processing Laboratory (LTS5), Ecole Polytechnique Fédérale de Lausanne, Switzerland
∗Institute of Sensors, Signals and Systems, Heriot-Watt University, UK
†Department of Radiology, University Hospital Center and University of Lausanne, Switzerland

ABSTRACT

This paper considers the problem of reconstructing ultrasound (US) element raw-data from random projections. It presents a new signal model, coined as *multi-channel ultrasound pulse-stream model*, which exploits the pulse-stream models of US signals and accounts for the inter-sensor dependencies. We propose a sampling theorem and a reconstruction algorithm, based on ℓ_1-minimization, for signals belonging to such a model. We show the benefits of the proposed approach through numerical simulations on 1D-signals and on in vivo carotid images.

Index Terms— Compressed sensing, sparsity, array imaging
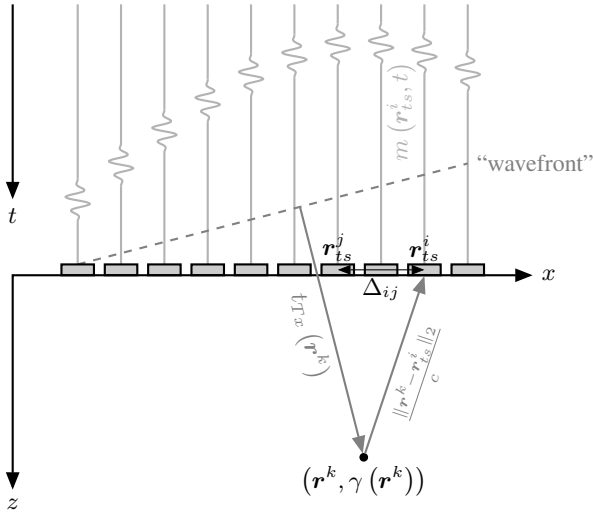
1. INTRODUCTION

Fig. 1: Standard 2D ultrasound imaging configuration.

The notion of *pulse stream* has been introduced by Hedge and Baraniuk [1] and designates signals that can be expressed as a convolution between a K-sparse spike train and a F-sparse impulse response.

Formally, let us consider a pulse stream $\boldsymbol{z} \in \mathbb{R}^N$, such that $\boldsymbol{z} = \boldsymbol{h} * \boldsymbol{s}$ with $\boldsymbol{s} \in \mathbb{R}^N$ the K-sparse spike train and $\boldsymbol{h} \in \mathbb{R}^N$ the F-sparse impulse response. The following Definition holds:

Definition 1 (Definition 2 of [1]). The pulse-stream model is defined as follows:

$$\mathcal{M}_{K,F}^z := \left\{ \boldsymbol{z} \in \mathbb{R}^N : \boldsymbol{z} = \boldsymbol{s} * \boldsymbol{h} \mid \boldsymbol{s} \in \mathcal{M}_K \text{ and } \boldsymbol{h} \in \mathcal{M}_F \right\}, \quad (1)$$

where $\mathcal{M}_K \subset \mathbb{R}^N$ and $\mathcal{M}_F \subset \mathbb{R}^N$ are restricted unions of L_K K-dimensional and L_F F-dimensional canonical subspaces, respectively.

For signals belonging to the pulse-stream model $\mathcal{M}_{K,F}^z$, Hedge and Baraniuk [1] have derived a sampling theorem where the number of measurements necessary for perfect reconstruction scales linearly with $K + F$ instead of KF (standard CS). In this work, we propose to extend the concept of pulse-stream models to array imaging, whose configuration is described on Figure 1. In such applications, the sensing process is divided into a transmit phase where one or several emitters are used to send a pulsed-wave in the medium, and a receive phase where the sensors receive medium response to the transmit wave. Such a configuration covers many applications such as medical ultrasound imaging, non-destructive testing, seismic imaging, sonar, lidar and synthetic aperture radar imaging.

Formally, let us assume that the array is made of N_{el} sensors, positioned at $\left(\boldsymbol{p}^i\right)_{i=1}^{N_{el}}$, as described on Figure 1. Let us also consider that the medium is made of K targets positioned at $\left(\boldsymbol{r}^k\right)_{k=1}^K$. The signal $m_i(t)$ received at the p-th element can be expressed as:

$$m_i(t) = \sum_{k=1}^K a_k h\left(t - t_i^k\right), \quad (2)$$

where a_k and t_i^k are the amplitude and delay associated with the k-th target and $h(t)$ is the received pulse, supposed to be known in the remainder of the paper. The delay associated with the k-th target depends on its relative position with respect to the sensor elements and can be expressed as follows:

$$t_i^k = t_{Tx}\left(\boldsymbol{r}^k\right) + \frac{||\boldsymbol{r}^k - \boldsymbol{p}^i||_2}{c}, \quad (3)$$

where c denotes the wave speed in the medium, supposed to be constant, and $t_{Tx}\left(\boldsymbol{r}^k\right)$ is the transmit delay which depends on the transmit phase settings.

This model have been extensively used in medical ultrasound imaging [2, 3, ?], non-destructive testing [?], radar imaging [?, 4]. Starting from the model described in Equation (2), we consider inter-channel dependencies in order to derive an additional structure of the array signals. This structure, expressed as restrictions on the possible support of the array signals, leads us to define a new model, denoted as *multi-channel array pulse streams*, from which we present a sampling theorem and a recovery algorithm.

The remainder of the paper is organized as follows. In Section 2, the signal model is presented, with the corresponding sampling theorem and recovery algorithm. Section 3 presents results on synthetic pulse streams as well as on simulated ultrasound images. Concluding remarks are given in Section 4.

2. SIGNAL MODELS FOR PULSE STREAMS IN ARRAY IMAGING

2.1. Channel recovery from a pulse-stream model

From Equation (2), one may express the signal $m_p(t)$ as $m_p(t) = (s * h)(t)$, where $s(t) = \sum_{k=1}^{K} a_k \delta\left(t - t_p^k\right)$ and $h(t)$ is the pulse.

Let us consider that the signal $m_p(t)$ is sampled at a rate f_s, leading to N samples $m_p(t^i)$, with $t^i = t^0 + i/f_s$ for $i \in \{1, \ldots, N\}$.

The vector $\boldsymbol{m}_p = \left[m_p(t^1), \ldots, m_p(t^N)\right]^T \in \mathbb{R}^N$ belongs to the pulse-stream model $\mathcal{M}_{K,F}^z$ where F denotes the size of the support of $\boldsymbol{h} \in \mathbb{R}^N$, supposed to be small compared to N and K the number of point-scatterers.

Thus, one may be able to sample array signals at a rate dictated by Hedge and Baraniuk [1] while ensuring a perfect recovery. Moreover, since the pulse is supposed to be known, the following convex problem can be solved to retrieve $\boldsymbol{m}_p$ from noisy measurements $\boldsymbol{y} = \Phi \boldsymbol{m}_p + \boldsymbol{n}$, with $\Phi \in \mathbb{R}^{M \times N}$ a Gaussian *i.i.d.* matrix:

$$\min_{\bar{\boldsymbol{s}}} \|\bar{\boldsymbol{s}}\|_1 \text{ subject to } \|\boldsymbol{y} - \Phi \mathsf{H} \bar{\boldsymbol{s}}\|_2 \leq \epsilon, \quad (4)$$

where H is a circulant matrix which contains time-shifted replicas of the pulse, $\boldsymbol{m}_p = \mathsf{H}\boldsymbol{s}$, $\boldsymbol{s}$ is the K-sparse spike train and ϵ is a higher bound of the ℓ_2-norm of the noise.

2.2. Multi-channel pulse-stream model

The model described in Section 2.1 is suited to single channel reconstructions. However, such a model does not account for inter-channel dependencies, which are self-evident in the proposed configuration (see Figure 1). By taking into account such dependencies, one may be able to decrease the number of measurements required to reconstruct array signals. The following theorem precises the way the dependencies between two channels may be expressed.

Theorem 1 (Two-channel scenario). *The support $\sigma(\boldsymbol{s}_i)$ of the spike train $\boldsymbol{s}_i$ corresponding to the sensor located at a distance Δ_{ij} from the sensor j, whose spike train is $\boldsymbol{s}_j$, has the following property:*

$$\sigma(\boldsymbol{s}_i) \subset S_{ij},$$

where $S_{ij} := \bigcup_{k=1}^{K} \Omega_k^{ij}$ is a union of $2D_{ij}$-dimensional subspaces Ω_k^{ij} defined by:

$$\Omega_k^{ij} := \{\{k - D_{ij}, \ldots, k + D_{ij}\}, \ k \in \sigma(\boldsymbol{s}_j)\},$$

where $D_{ij} = \lceil f_s \Delta_{ij}/c \rceil$.

In the above theorem, $\lceil . \rceil$ designates the round value.

Proof. Let us suppose that $x_j(t) = \sum_{k=1}^{K} a_k \delta\left(t - t_j^k\right)$ and $x_i(t) = \sum_{k=1}^{K} a_k \delta\left(t - t_i^k\right)$. From Equation (3), one may deduce the following:

$$\begin{aligned}
t_j^k &= t_{Tx}\left(\boldsymbol{r}^k\right) + t_{Rx}\left(\boldsymbol{r}^k, \boldsymbol{r}_{ts}^j\right) \\
&= t_{Tx}\left(\boldsymbol{r}^k\right) + \frac{\|\boldsymbol{r}^k - \boldsymbol{r}_{ts}^j\|_2}{c} \\
&\leq t_{Tx}\left(\boldsymbol{r}^k\right) + \frac{\|\boldsymbol{r}^k - \boldsymbol{r}_{ts}^i\|_2}{c} + \frac{\Delta_{ij}}{c} \\
&\leq t_i^k + \frac{\Delta_{ij}}{c}.
\end{aligned}$$

Reversely, one can deduce that $t_j^k \geq t_i^k - \frac{\Delta_{ij}}{c}$, which leads to $t_i^k \in \left[t_j^k - \frac{\Delta_{ij}}{c}, t_j^k + \frac{\Delta_{ij}}{c}\right]$. Thus, by multiplying by f_s, one may deduce that:

$$\forall l \in \sigma(\boldsymbol{s}_i), \exists p \in \sigma(\boldsymbol{s}_j) \mid l \in \{p - D_{ij}, \ldots, p + D_{ij}\}, \quad (5)$$

where $D_{ij} = \lceil f_s \Delta_{ij}/c \rceil$. Generalizing Equation (5) to the support of $\sigma(\boldsymbol{s}_i)$, one may retrieve the result of Theorem 1. $\square$

Theorem 1 states that the support of $\boldsymbol{s}_i$ is a union of K $2D_{ij}$-dimensional subspaces located around the support $\sigma(\boldsymbol{s}_j)$ of the signal received at sensor j. The dimension of each subspace depends on the distance between the sensors.

We can go further than the two-channel scenario by considering that we have prior knowledge on multiple channels. In this case, the following theorem holds.

Theorem 2 (Multi-channel scenario). *The support $\sigma(\boldsymbol{s}_i)$ of the spike train $\boldsymbol{s}_i$ corresponding to the sensor located at distances $(\Delta_{ij})_{j=1}^n$ from a set of n sensors, whose spike trains are $(\boldsymbol{s}_j)_{j=1}^n$, has the following property:*

$$\sigma(\boldsymbol{s}_i) \subset S,$$

where $S := \bigcap_{j=1}^{n} S_{ij}$ is the intersection of the spaces S_{ij} defined in Theorem 1.

Proof. This is a simple generalization of Theorem 1. Let us denote as $(\boldsymbol{s}_j)_{j=1}^n$ the spike trains associated with the n considered sensors. Then, Theorem 1 states that:

$$\forall j \in \{1, \ldots, n\}, \ \sigma(\boldsymbol{s}_i) \in S_{ij}$$
$$\Leftrightarrow \sigma(\boldsymbol{s}_i) \in \bigcap_{j=1}^{n} S_{ij}.$$

$\square$

In this case, the support $\sigma(\boldsymbol{s}_i)$ is included into a smaller subspace, taking into account the dependencies between the considered sensor and the n other ones. We use the result of Theorem 2 to define the multi-channel pulse-stream model as:

$$\mathcal{U}_{K,F}^z := \left\{\boldsymbol{z} \in \mathbb{R}^N : \boldsymbol{z} = \boldsymbol{s} * \boldsymbol{h} \mid \boldsymbol{s} \in \mathcal{M}_K, \ \sigma(\boldsymbol{s}) \subset S\right\}, \quad (6)$$

where $\boldsymbol{h}$ is supposed to be known.

2.3. Sampling theorem for multi-channel pulse-stream signals

The multi-channel pulse-stream model has an additional structure compared to the single-channel pulse-stream model, *i.e.* $\mathcal{U}^z_{K,F} \subset \mathcal{M}^z_{K,F}$, which can be exploited in order to reduce the sampling rate requirements for signals belonging to $\mathcal{U}^z_{K,F}$. The theorem hereafter makes this precise and sets the sampling requirement.

Theorem 3. *Suppose that $\mathcal{U}^z_{K,F}$ is the multi-channel pulse-stream model defined in Equation* (6). *Let $t > 0$ and $\delta > 0$. Choose a $M \times N$ i.i.d Gaussian matrix Φ with*

$$M \geq \mathcal{O}\left((K+F)\ln\left(\frac{1}{\delta}\right) + K\left(1 + \log\left(\frac{|S|}{K}\right)\right) + t\right).$$

Then Φ satisfies the following property with probability $1 - e^{-t}$: $\forall z_1, z_2 \in \mathcal{U}^z_{K,F}$,

$$(1-\delta)\|z_1 - z_2\|^2 \leq \|\Phi z_1 - \Phi z_2\|^2 \leq (1+\delta)\|z_1 - z_2\|^2.$$

In the theorem above $|S|$ denotes the cardinality of the set S.

Proof. The proof is based on Theorem 1 of [1]. Suppose that $z \in \mathcal{U}^z_{K,F}$, then, $z \in \mathcal{M}^z_{K,F}$. From [1], one may set the bound M as:

$$M \geq \mathcal{O}\left((K+F)\ln\left(\frac{1}{\delta}\right) + \log(L_K L_F) + t\right) \quad (7)$$

where $t > 0$. When h is known, $L_F = 1$. Moreover, if we consider that $\sigma(s) \subset S$, then the following inequality holds:

$$L_K \leq \binom{|S|}{K} \approx \left(\frac{e|S|}{K}\right)^K$$

$$\Leftrightarrow \log(L_K) \leq K\left(1 + \log\left(\frac{|S|}{K}\right)\right).$$

Introducing the above results in Equation (7) leads to the results of Theorem 3. □

The main benefit of Theorem 3 is that the number of measurements required for perfect reconstruction are $\mathcal{O}(K\log(|S|/K))$, instead of $\mathcal{O}(K\log(N/K))$ in the case of the single-channel pulse stream model.

Theorem 3 can be interpreted in light of the D-RIP property introduced by Candes *et al.* [5]. Indeed, a signal $z \in \mathcal{U}^z_{K,F}$ is K-sparse in a convolutional (coherent) dictionary formed by shifted replica of the pulse h, and can be acquired with $\mathcal{O}(K\log(N/K))$ Gaussian i.i.d. measurements [5]. In addition, $z \in \mathcal{U}^z_{K,F}$ implies that $\sigma(s) \in S$ which means that the recovery problem can be solved on $\mathbb{R}^{|S|}$ rather than $\mathbb{R}^N$ and, consequently, that the signal can be acquired with $\mathcal{O}(K\log(|S|/K))$ Gaussian i.i.d. measurements.

2.4. Recovery of multi-channel pulse-stream signals

The signal $m = s * h$, $m \in \mathcal{U}^z_{K,F}$ can be written as $m = Hs$, where $H \in \mathbb{R}^{N \times N}$ is a convolution matrix which exhibits a Toeplitz structure. Let us consider that the signal $y = \Phi m$ is measured, where $\Phi \in \mathbb{R}^{M \times N}$ satisfies the requirements of Theorem 3.

As described in Section 2.3, the recovery problem in $\mathbb{R}^N$ can be recast as the following recovery problem in $\mathbb{R}^{|S|}$:

Find $\alpha \in \mathbb{R}^{|S|}$ such that $||y - (\Phi H)_{|S}\,\alpha||_2 \leq \epsilon$, $||\alpha||_0 = K$, (8)

where $\epsilon \in \mathbb{R}_+$ accounts for the noise level and $(\Phi H)_{|S} \in \mathbb{R}^{M \times |S|}$ corresponds to a submatrix of (ΦH) formed by the columns indexed by the support S. Depending on the ratio between the number of measurements M and the size of the support S and the noise level, two different recovery procedures may be considered.

2.4.1. Recovery by least-square minimization

When $M \leq |S|$ and $\epsilon = 0$, Problem (8) involves an overcomplete matrix $(\Phi H)_{|S} \in \mathbb{R}^{M \times |S|}$ and can be solved by least-square minimization. In this case, the solution $\alpha^\star$ of Problem (8) is expressed as:

$$\alpha^\star = (\Phi H)^\dagger_{|S}\,y, \quad (9)$$

where $(\Phi H)^\dagger_{|S}$ denotes the Moore pseudo-inverse of $(\Phi H)_{|S}$.

2.4.2. Recovery by ℓ_1-minimization on the signal support

In a more general case, $\alpha^\star$ can be recovered by solving the following convex optimization problem [5]:

$$\min_{\alpha} \|\alpha\|_1 \text{ subject to } \|y - (\Phi H)_{|S}\,\alpha\|_2 \leq \epsilon. \quad (10)$$

Problem (10) is solved using state-of-the-art convex optimization algorithms.

3. EXPERIMENTS

We now present the results of experiments that validate the proposed approach and show its benefits. In all the experiments, Problem (10) is solved using the alternating direction methods of multipliers (ADMM) [6].
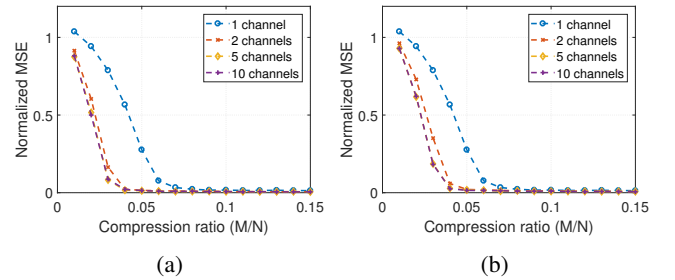
3.1. Synthetic $1D$-pulse streams

Fig. 2: Normalized MSE for (a) $\Delta = 0.31\,\text{mm}$ (phased-array) and (b) $\Delta = 0.62\,\text{mm}$ (linear-array) vs. the compression ratio (M/N) for the proposed method for 1-, 2-, 5- and 10-channel scenarios. Signals parameters: $N = 2000$, $F = 31$, $K = 20$.

First, $K = 20$ point-scatterers with random amplitudes and positions are generated. 10 sensors are considered, with an inter-sensor spacing of Δ. Pulse-streams of length $N = 2000$ are simulated mimicking ultrasound plane-wave imaging with normal incidence [7]. The considerd pulse $h(t)$ is a convolution between a 2-cycle square excitation signal with a Gaussian pulse which mimicks the impulse response of ultrasound transducer elements (2.5 cycles, central frequency 5.208 MHz, bandwidth 67 %). The sampling frequency f_s is set to 20.8 MHz.
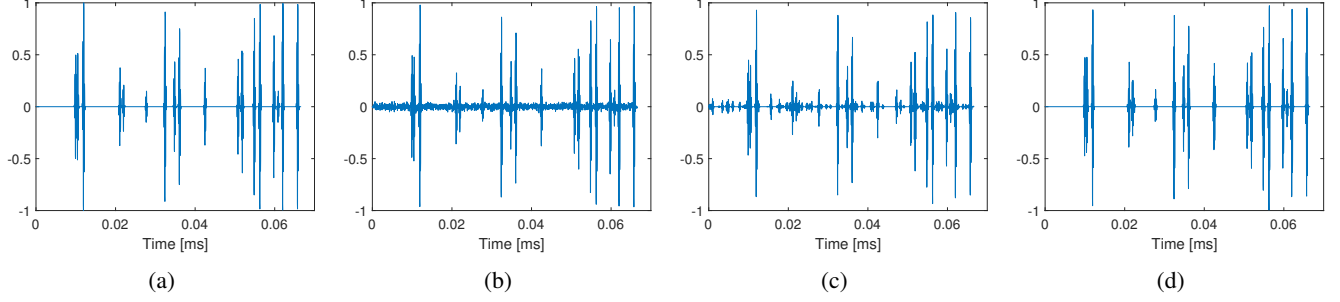
Fig. 3: (a) Original signal (b) Noisy signal (SNR =40 dB) (c) Recovered estimate from $M = 160$ measurements in a 1-channel scenario (d) Recovered estimate from $M = 160$ measurements in a 5-channel scenario.

Figure 2 displays the averaged results of a Monte-Carlo simulation over 1000 trials of the ADMM algorithm. Each trial was conducted by randomly generating the amplitudes and positions of the K point-scatterers, the Gaussian i.i.d. matrix $\Phi \in \mathbb{R}^{M \times N}$ and by reconstructing the raw data $\boldsymbol{m}$ of one sensor from different values of M/N. 1-channel as well as multi-channel scenarios are considered. For the multi-channel scenarios, prior knowledge on the support of the spike trains of $1, 4$ and 9 neighboring sensors of the sensor of interest are considered. Figure 2a and 2b show the normalized mean squared error (NMSE), calculated as $\|\boldsymbol{m} - \boldsymbol{m}^\star\|_2 / \|\boldsymbol{m}\|_2$, where $\boldsymbol{m}$ is the reference and $\boldsymbol{m}^\star$ the estimate, for two different inter-sensor spacings, namely $0.31\,\mathrm{mm}$ (one wavelength) and $0.62\,\mathrm{mm}$ (two wavelengths). Regarding the optimization algorithm, the maximum number of iterations is set to 1000 and $\epsilon = 0$.

From Figure 2, it is clear that the multi-channel configurations outperform the 1-channel configuration. Regarding Figures 2a and 2b, it can be noticed that, for a higher inter-sensor spacing, the 5-channel and 10-channel scenarios outperform the 2-channel scenario. Indeed, when the spacing is higher, the dimension of the subspaces S_i is increased and the dimensionality reduction induced by Theorem 2 has a higher impact.

Figure 3 demonstrates that the proposed algorithm is robust to small amount of noise (SNR = 40 dB). For this experiment, the settings are the same as the ones used for the noiseless experiment. A small amount of Gaussian noise is added to the element raw-data of each sensor, leading to the signal displayed on Figure 3b. Figures 3c and 3d show the recovered signals for the 1-channel and 5-channels scenarios, respectively, for a number of measurements $M = 160$. It can be seen that the signal recovered from the 5-channel scenario is closer to the original signal than the one recovered from the 1-channel scenario.

3.2. *In vivo* ultrasound images

Element raw-data of an *in vivo* carotid, for 1 PW insonification with normal incidence, have been acquired with an Ultrasonix scanner (Ultrasonix Analogic Ultrasound, Richmond, BC, Canada), equipped with a linear probe composed of 128 transducer-elements, working at 5 MHz with 100 % bandwidth, with an inter-sensor spacing of 0.46 mm. The sampling frequency has been set to 40 MHz.

After acquisition, the element raw-data are imported on MATLAB (The Mathworks, Natic, MA) and compressed using a Gaussian *i.i.d* matrix $\Phi \in \mathbb{R}^{M \times N}$, with a compression ratio $M/N = 0.06$, with $N = 1519$. The pulse is supposed to be known and equal to the one described in Section 3.1. In the multi-channel scenario, a sequential reconstruction is achieved where each channel is recovered with prior knowledge on the support of the spike train

corresponding to the neighbouring channel (obtained from the previous reconstruction). Concerning the optimization algorithm, the maximum number of iterations is set to 2000 and $\epsilon = 0.3\|\boldsymbol{y}\|_2$.

Once the raw data are reconstructed from compressed measurements, standard US beamforming is applied to generate the radio-frequency (RF) image. The envelope is extracted through Hilbert transform, normalized and log-compressed (dynamic range of 40 dB) to obtain the B-mode image.

Figure 4, which displays the recovered B-mode images, shows an increase of the image quality in the multi-channel scenario. This increase is quantified by a difference of 1 dB in the peak-signal-to-noise ratio (PSNR) between the 1- and the multi-channel reconstructions.
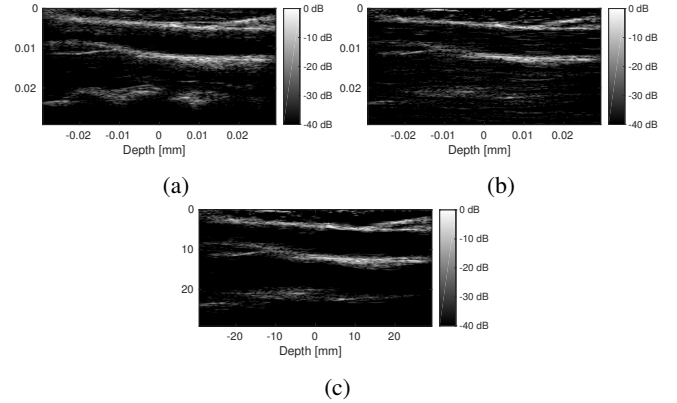

Fig. 4: (a) Original B-mode image of the carotid; Recovered B-mode image from $M = 91$ measurements (b) in a 1-channel scenario (PSNR = 28.4 dB); (c) in a 2-channels scenario (PSNR = 29.4 dB).

4. CONCLUSION

In this paper, we have presented an extension of the pulse-stream model to ultrasound imaging. The proposed model, coined as *multi-channel US pulse-stream model*, accounts for the inter-sensor dependencies as an additional structure to the general pulse-stream model. This structure enables us to quantitatively estimate the number of random projections necessary to sample such signals. We also suggest a reconstruction method based on ℓ_1-minimization on the reduced signal support. We have illustrated its benefits on synthetic $1D$-pulses as well as on *in vivo* ultrasound images.

5. REFERENCES

[1] Chinmay Hegde and Richard G. Baraniuk, "Sampling and recovery of pulse streams," *IEEE Trans. Signal Process.*, vol. 59, no. 4, pp. 1505–1517, apr 2011.

[2] Tanya Chernyakova and Yonina C. Eldar, "Fourier-domain beamforming: the path to compressed ultrasound imaging," *IEEE Trans. Ultrason. Ferroelectr. Freq. Control*, vol. 61, no. 8, pp. 1252–1267, aug 2014.

[3] Ronen Tur, Yonina C. Eldar, and Zvi Friedman, "Innovation rate sampling of pulse streams with application to ultrasound imaging," *IEEE Trans. Signal Process.*, vol. 59, no. 4, pp. 1827–1842, apr 2011.

[4] Richard Baraniuk and Philippe Steeghs, "Compressive radar imaging," in *IEEE Natl. Radar Conf. - Proc.*, 2007, pp. 128–133.

[5] Emmanuel J Candes, Yonina C Eldar, Deanna Needell, and Paige Randall, "Compressed sensing with coherent and redundant dictionaries," *Appl. Comput. Harmon. Anal.*, vol. 31, no. 1, pp. 59–73, jul 2011.

[6] Stephen Boyd, "Distributed optimization and statistical learning via the alternating direction method of multipliers," *Found. Trends Mach. Learn.*, vol. 3, no. 1, pp. 1–122, jan 2011.

[7] Gabriel Montaldo, Mickaël Tanter, Jérémy Bercoff, Nicolas Benech, and Mathias Fink, "Coherent plane-wave compounding for very high frame rate ultrasonography and transient elastography," *IEEE Trans. Ultrason. Ferroelectr. Freq. Control*, vol. 56, no. 3, pp. 489–506, mar 2009.